

Greater Bone Formation of Y2 Knockout Mice Is Associated with Increased Osteoprogenitor Numbers and Altered Y1 Receptor Expression^{*[5]}

Received for publication, October 12, 2006, and in revised form, April 17, 2007. Published, JBC Papers in Press, May 9, 2007, DOI 10.1074/jbc.M609629200

Pernilla Lundberg^{†1,2}, Susan J. Allison^{§1}, Nicola J. Lee[‡], Paul A. Baldock[§], Nathalie Brouard[¶], Stephanie Rost[‡], Ronaldo F. Enriquez[§], Amanda Sainsbury[‡], Meriem Lamghari[‡], Paul Simmons[¶], John A. Eisman[§], Edith M. Gardiner^{||}, and Herbert Herzog^{‡3}

From the [†]Neuroscience Research Program and the [§]Bone and Mineral Research Program, Garvan Institute of Medical Research, St. Vincent's Hospital, 384 Victoria St., Darlinghurst, Sydney, New South Wales 2010, the [¶]Stem Cell Research Laboratory, Peter MacCallum Cancer Institute, Melbourne, Victoria 8006, and the ^{||}Diamantina Institute, University of Queensland, Princess Alexandra Hospital, Ipswich Road, Brisbane, Queensland 4102, Australia

Germ line or hypothalamus-specific deletion of Y2 receptors in mice results in a doubling of trabecular bone volume. However, the specific mechanism by which deletion of Y2 receptors increases bone mass has not yet been identified. Here we show that cultured adherent bone marrow stromal cells from Y2^{-/-} mice also demonstrate increased mineralization *in vitro*. Isolation of two populations of progenitor cell types, an immature mesenchymal stem cell population and a more highly differentiated population of progenitor cells, revealed a greater number of the progenitor cells within the bone of Y2^{-/-} mice. Analysis of Y receptor transcripts in cultured stromal cells from wild-type mice revealed high levels of Y1 but not Y2, Y4, Y5, or y6 receptor mRNA. Interestingly, germ line Y2 receptor deletion causes Y1 receptor down-regulation in stromal cells and bone tissue possibly due to the lack of feedback inhibition of NPY release and subsequent overstimulation of Y1 receptors. Furthermore, deletion of Y1 receptors resulted in increased bone mineral density in mice. Together, these findings indicate that the greater number of mesenchymal progenitors and the altered Y1 receptor expression within bone cells in the absence of Y2 receptors are a likely mechanism for the greater bone mineralization *in vivo* and *in vitro*, opening up potential new treatment avenues for osteoporosis.

A role for the neuropeptide Y (NPY)⁴ receptor system in the regulation of bone formation was first revealed with the dem-

onstration that germ line deletion of Y2 receptors resulted in increased bone formation in the distal femur of mice. This increase in bone formation was due to elevated osteoblast activity and resulted in a 2-fold greater trabecular bone volume and significantly elevated cortical bone mass compared with wild-type mice (1, 2). Interestingly, conditional deletion of Y2 receptors solely from the hypothalamus of adult mice produced a comparable increase in bone volume within just 5 weeks, demonstrating this to be a potent and centrally mediated pathway (1, 2). However, the mechanism by which ablation of either germ line or hypothalamic Y2 receptors stimulates osteoblast activity to increase bone formation is not yet known.

The control of bone remodeling has been traditionally thought to be regulated primarily by endocrine systems and by locally acting factors such as cytokines and growth factors. However, this view is gradually changing with increasing evidence that neuronal factors are also able to modify the activity of bone cells. The presence of nerve fibers and neuronal factors within bone tissue has been demonstrated by a number of studies (3, 4). Furthermore, retrograde tracing studies have demonstrated that neuronal input into bone tissue has connections to the hypothalamus, consistent with the demonstration that conditional Y2 receptor deletion in the hypothalamus is capable of altering bone formation (1, 5).

NPY-immunoreactive fibers have been shown within bone marrow, periosteum, and bone tissue, preferentially associated with vascular elements, with some located around bone lining and marrow cells (3, 6–10). The direct modulation of bone cell activity by various neuronal factors has also been demonstrated *in vitro*. Peptides such as calcitonin gene-related peptide and substance P, as well as calcitonin gene-related peptide receptors and neurokinin-1 receptors are located on bone cells and have been demonstrated to modify bone cell function (11–15). Other neuropeptides in addition to NPY have also been identified within bone tissue. For example, the presence of vasoactive intestinal peptide receptors has been demonstrated on both these cell types and vasoactive intestinal peptide has been shown to regulate the activity of both osteoblasts and oste-

sorting; CFU, colony forming unit; PBS, phosphate-buffered saline; MACS, magnetic activated cell sorting; BMC, bone mineral content; BMD, bone mineral density.

* This work was supported by the National Health and Medical Research Council (NHMRC) (Project Grant 276412), an NHMRC scholarship (to S. J. A.), NHMRC fellowships (to H. H. and A. S.), and a fellowship (to P. L.) from The Swedish Society for Medical Research. The costs of publication of this article were defrayed in part by the payment of page charges. This article must therefore be hereby marked "advertisement" in accordance with 18 U.S.C. Section 1734 solely to indicate this fact.

[5] The on-line version of this article (available at <http://www.jbc.org>) contains supplemental Fig. S1 and Table S1.

¹ Both authors contributed equally to this work.

² To whom correspondence may be addressed: Current address; Dept. of Odontology, Section for Oral Cell Biology, Umea University, Umea SE-901 87, Sweden. Tel.: 46-90-785-6294; Fax: 46-90-13-9289; E-mail: pernilla.lundberg@odont.umu.se.

³ To whom correspondence may be addressed: Tel.: 61-2-9295-8296; Fax: 61-2-9295-8281; E-mail: h.herzog@garvan.org.au.

⁴ The abbreviations used are: NPY, neuropeptide Y; MSC, mesenchymal stem cell; Sca-1, stem cell antigen-1; FACS, fluorescence-activated cell

oclasts (12, 16–18). Recent studies have revealed that the central antiosteogenic action of leptin is mediated via the sympathetic nervous system, whereas β -adrenergic receptors have been identified on osteoblasts and osteoblast-like cell lines from human, rat, and mouse (19–21). The presence of neural factors and their receptors within bone cells and their ability to modulate bone cell activity therefore support a potential physiological role for neural factors in the regulation of bone function.

The bone-forming osteoblasts originate from mesenchymal stem cells (MSCs), a multipotential cell type that is also able to give rise to adipocytes and chondrocytes (22–24). The isolation and characterization of MSCs has proven to be difficult due to their rarity within bone, lack of knowledge of their localization within bone, and the lack of specific markers for their identification (25). Various methods have been utilized by different groups to isolate a homogenous population of multipotential mesenchymal progenitors from mice. For example, the immunodepletion of hematopoietic cells following plastic adhesion of stromal cells resulted in a population of cells that expressed stem cell antigen-1 (Sca-1), an antigen previously associated with hematopoietic cells, and were subsequently demonstrated to exhibit adipogenic, chondrogenic, and osteogenic potential (26, 27). Selection based on 5-fluorouracil resistance and fluorescence-activated cell sorting (FACS) using wheat germ agglutinin and Sca-1 was used for the identification of a candidate osteoprogenitor cell population in mouse bone marrow (28). A method to isolate an immature stromal progenitor cell population from the tissue surrounding bone marrow by depletion of hematopoietic cells followed by cell sorting to isolate Sca-1⁺ cells was recently developed in one of our laboratories. This cell population exhibited properties of mesenchymal stem cells, being highly proliferative with a high capacity to form colony forming units (CFUs) and exhibiting multipotentiality, with the ability to differentiate down osteoblastic, adipogenic, and chondrocytic lineages (25). Furthermore, additional sorting of the Sca-1⁺ population of cells using an antibody recognizing CD51 eliminated CD51⁺ erythroid precursor cell types and yielded a more mature “osteoprogenitor” cell population.

Here we have investigated whether a change in the osteoprogenitor cell population may contribute to the greater bone formation and bone volume of the Y2 receptor-deficient models. We reasoned that a change in the release of factors may affect the number or the ability of bone-forming precursor cells to develop into mature mineral-producing osteoblasts. To test this we evaluated the ability of bone marrow stromal cells from Y2^{-/-} mice to produce mineral *in vitro*. We also assessed the number of mesenchymal and progenitor cells in these mice. Furthermore, we investigated whether Y receptors are expressed in this stromal cell population and whether an alteration in Y receptor expression may also constitute a mechanism by which deletion of Y2 receptors leads to increased bone formation *in vivo*. The results revealed that down-regulation of local Y1 receptor signaling may provide a mechanism for the greater bone formation of the Y2^{-/-} model.

EXPERIMENTAL PROCEDURES

Animal experiments were approved by the Garvan/St. Vincent's Animal Experimentation Ethics Committee and were conducted in accordance with relevant guidelines and regulations.

Generation of Y1^{-/-} and Y2^{-/-} Mutant Mice—Germ line deletion of Y1 and Y2 receptor genes (*Npy1r* and *Npy2r*, respectively) was achieved as previously described (29, 30), by crossing Y1 and Y2 receptor-floxed mice (Y1^{lox/lox} and Y2^{lox/lox}) with oocyte-specific Cre-recombinase-expressing C57/BL6 mice (31), resulting in the removal of the entire coding region of the Y1 or Y2 gene.

Isolation of Bone Marrow Stromal Cells—To isolate plastic-adherent bone marrow stromal cells, 5- to 9-week-old male wild-type and germ line Y2^{-/-} mice were sacrificed by cervical dislocation, and marrow was flushed from femurs and tibias with α -minimal essential medium containing 10% fetal bovine serum, 2 mM L-glutamine, 2.2g/liter sodium bicarbonate, 0.017 M HEPES, 100 IU/ml, 100 μ g/ml penicillin/streptomycin, and 34,000 IU/ml, 34 mg/liter gentamycin (Control media). Cells were plated at a density of 1.9×10^6 cells/cm² in 50-cm² plastic tissue culture plates (BD Biosciences Labware, Franklin Lakes, NJ) and maintained at 37 °C with 5% humidified CO₂. The non-adherent cell population was removed after 72 h by a medium change. Cells were trypsinized 4 days later (0.25% trypsin containing 0.53 mM EDTA) and re-plated at 6.6×10^4 cells/cm² in control media. Cells were changed into differentiation media 2 days later.

Differentiation of Bone Marrow Stromal Cell Cultures—Differentiation into adipocytes and mineral-producing osteoblasts was achieved by using adipogenic (control α -minimal essential medium media with 5 μ g/ml insulin and 10 nM dexamethasone) or osteogenic media (control α -minimal essential medium media with 50 mg/liter ascorbic acid and 10 mM β -glycerol phosphate), respectively.

Staining of Bone Marrow Stromal Cells for Assessment of Osteoblast and Adipocyte Differentiation—Cells were fixed in 2% paraformaldehyde for 10 min at room temperature. Osteoblast differentiation and mineralization of extracellular matrix were visualized by von Kossa staining with 2% silver nitrate under UV light for 30 min. The extent of mineralization was assessed using the Leica QWin imaging system (Leica Microsystems, Heerbrugg, Switzerland). Formation of adipocytes was visualized using Oil Red-O (12% Oil Red-O, 60% isopropanol). The extent of adipogenic differentiation was assessed by counting the number of cells containing well stained oil droplets in 10 random low power visual fields using the QWin imaging system.

RNA Extraction and Reverse Transcription-PCR Analysis of Cultured Bone Marrow Stromal Cells—RNA was isolated from cultures of bone marrow stromal cells in 12-well plates using TRIzol[®] reagent as per the manufacturer's instructions. reverse transcription-PCR was performed with TaqDNA polymerase (Roche Applied Science) using 1 μ l of cDNA synthesized from 1 μ g of total RNA with oligo(dT)₂₀ by using the SuperScript III First-Strand Synthesis System for reverse transcription-PCR (Invitrogen). The specific primers and annealing temperatures

Greater Osteoprogenitor Number of Y2 Knockout Mice

used along with the resultant product size obtained are as follows: mY1 receptor (323 bp, 55 °C, forward: 5'-CTCGCTGGTTCTCATCGCTGTGGAACGG-3', reverse: 5'-GCGAATGTATATCTTGAAGTAG-3'), mY2 receptor (520 bp, 60 °C, forward: 5'-TCCTGGATTCCATCTGAG-3', reverse: 5'-GGTCCAGAGCAATGACTGTC-3'), mY4 receptor (367 bp, 56 °C, forward: 5'-TCTACAGACAGTAGACCAGG-3', reverse: 5'-GTAGGTTGGTTCACATTGGAC-3'), mY5 receptor (204 bp, 60 °C, forward: 5'-GGGCTCTATACATTTGTAAGTCTTCTGGG-3', reverse: 5'-CATGGCTTTGCCGAACATCCACTGATCC-3'), mY6 receptor (347 bp, 56 °C, forward: 5'-GGAGGGATGGTTATTGTGAC-3', reverse: 5'-GTTGTGCTCTTGCCACTGG-3'), and mouse glyceraldehyde-3-phosphate (269 bp, 57 °C, forward: 5'-ACTTTGTCAAGCTCATTTCC-3', reverse: 5'-TGCAGCGAACTTTATTGATG-3'). PCR reactions were performed for the number of cycles indicated with denaturing at 94 °C and extension at 72 °C.

Quantitative Real-time PCR—Expression of the osteoblast-specific markers alkaline phosphatase and osteocalcin and the adipocyte marker peroxisome proliferator-activated receptor- γ were analyzed by quantitative real-time PCR using the TaqMan Universal PCR master mix (Applied Biosystems, Foster City, CA) and a sequence detection system (ABI Prism 7900 HT Sequence Detection System and Software, Applied Biosystems) with fluorescence-labeled probes (reporter fluorescent dye VIC at the 5'-end and quencher fluorescent dye tetramethylrhodamine at the 3'-end). The specific primers and probes used are as follow for β -actin (sense: 5'-GGACCTGACGGACTACCTCATG-3', antisense: 5'-TCTTTGATGTCACGCACGATTT-3', probe: 5'-CCTGACCGAGCGTGGCTACAGCTTC-3'), osteocalcin (sense: 5'-GGAGGGCAATAAGGTAGTGAACA-3', antisense: 5'-CACAAGCAGGGTTAAGCTCACA-3', probe: 5'-CGGCCTACCTTGAGCCCTCAGTC-3'), and alkaline phosphatase (sense: 5'-GGACTGGTACTCGGATAACGAGAT-3', antisense: 5'-ACATCAGTTCGTTTCTTCGGGTACA-3', probe: 5'-CGCCACCCATGATCACGTCGATATC-3'). Primers and probes for peroxisome proliferator-activated receptor- γ were analyzed using an inventoried kit from Applied Biosystems. To control variability in amplification due to differences in starting mRNA concentrations, β -actin was used as an internal standard. The relative expression of target mRNA was computed from the target Ct values and the β -actin C_t value using the standard curve method (User Bulletin 2, Applied Biosystems).

In Situ Hybridization—Antisense and sense Riboprobes for the mouse Y1 receptor were generated from a cDNA region corresponding to bases 60–653 of the coding sequence (where 1 represents the first base of the translation initiation codon) subcloned into pBluescript plasmid vector (Stratagene). Probes were labeled with digoxigenin-UTP by *in vitro* transcription with either T3 (antisense probe) or T7 (sense probe) RNA polymerase using a DIG RNA labeling kit (Roche Applied Science) according to the manufacturer's instructions. Riboprobes were purified from unincorporated label using Sephadex G-25 spin columns, and their yield was assessed by dot blot.

In situ hybridization was carried out as previously described with minor modifications (32) on 5- μ m sections of decalcified bone. All procedures were carried out at room temperature

unless specified otherwise. Sections were dewaxed in xylene, rehydrated through decreasing concentrations of ethanol (100% to 70%), and then fixed in 2% paraformaldehyde in PBS on ice for 10 min. After washing in PBS, sections were incubated at 37 °C with proteinase K (Roche Applied Science) at a concentration of 5 μ g/ml in 50 mM Tris-HCl (pH 7.5) and 5 mM EDTA for 20 min, followed by 0.1 M glycine in PBS for 5 min. Sections were acetylated with 1 \times triethanolamine containing 0.25% (v/v) acetic anhydride for 10 min and washed in PBS before hybridization.

Hybridization was carried out overnight at 45 °C in a humid environment. Sections were incubated with hybridization solution containing 50% formamide, 5 \times SSC, 250 μ g/ml salmon sperm DNA, 250 μ g/ml yeast tRNA, 1 \times Denhardt's solution, 10% dextran sulfate, 10 mM dithiothreitol, and 200 ng/ml digoxigenin-labeled Riboprobe. The sections were washed in 2 \times SSC for 5 min followed by 0.2 \times SSC at 62 °C for 30 min and 0.1 \times SSC at 65 °C for 30 min. They were then incubated with 20 μ g/ml RNase A (Roche Applied Science) in 0.5 M NaCl, 10 mM Tris-HCl, and 1 mM EDTA at 37 °C for 15 min followed by washes with 2 \times SSC for 5 min, 0.1 \times SSC at 37 °C for 30 min. Following the washes, antidigoxigenin Fab antibody fragments conjugated with alkaline phosphatase (Roche Applied Science) and nitro blue tetrazolium/5-bromo-4-chloro-3-indolyl phosphate stock solution (Roche Applied Science) containing 1 mM levamisole were used for colorimetric detection following the manufacturer's instructions.

Isolation of Mesenchymal Stem and Osteoprogenitor Cells—Femurs, tibias, and iliac crests from 8- to 15-week-old male mice were dissected and thoroughly cleaned of muscle and connective tissue, after which the outer surface of the bones was scraped to remove the periosteal surface. Long bones and iliac crests were crushed using a mortar and pestle in washing buffer (2% fetal bovine serum in PBS), then cut up finely in 3 mg/ml Worthington collagenase type 1. Bone fragments were then collagenase-digested for 45 min at 300 rpm at 37 °C. Following digestion, large fragments were removed by filtration (70- μ m nylon mesh cell strainer, BD Biosciences). Cells were collected by centrifugation (1000 rpm, 4 min) and resuspended in 2 ml of washing buffer, and the viable cell number was counted using trypan blue.

Contaminating hematopoietic cells were removed by lineage depletion using magnetic activated cell sorting (MACS) microbeads. Cells were incubated with a mixture consisting of the purified antibodies against B220, Gr-1, Mac-1, CD4, CD8, CD3, CD5 (all 1:500 dilution), and TER119 (1:1000 dilution) (BD Pharmingen) diluted in washing buffer for 20 min at 4 °C. Excess antibody was removed by centrifugation, and the cell suspension was then incubated with MACS[®] goat anti-rat IgG magnetic microbeads (20 μ l per 10⁷ cells, Miltenyi Biotech, Bergisch-Gladbach, Germany) diluted in washing buffer for 15 min at 4 °C. The cell suspension containing the bound magnetic beads was then applied to a VarioMACS[®] separator with an LS MACS[®] Cell Separation Column (Miltenyi Biotech). Eluted negatively selected cells devoid of hematopoietic cells were collected, centrifuged at 1200 rpm for 4 min, and resuspended in 500 μ l of washing buffer, and viable cells were counted using trypan blue.

To prepare for cell sorting for selection of MSCs and progenitor cells, cells ($\sim 3 \times 10^6$) were incubated for 20 min at 4 °C with 2.5 μ l each of the biotinylated or fluorescein isothiocyanate- or phycoerythrin-conjugated antibodies against the surface markers Sca-1, CD45 (BD Pharmingen), CD31, and CD51 (BD Biosciences). Appropriate controls (no antibody, isotype control using nonspecific IgG, fluorescein isothiocyanate, phycoerythrin, biotinylated, and all antibodies) were also set up by incubation of 0.5 μ l of antibody with $\sim 20,000$ cells for each control group. The secondary fluorescein allophycocyanin-conjugated streptavidin (1:500 dilution, BD Biosciences) was then added to all tubes containing the biotinylated-CD51 antibody (CD51 control tube, all antibodies, and experimental samples), incubated for a further 15 min at 4 °C. 7-Amino-actinomycin D (1:300 dilution, BD Biosciences) was used to detect non-viable cells. Cells were then sorted using a FACS Vantage SETM (BD Biosciences) with FACSDiva SETM software version 4.1.2 (BD Biosciences) using a nozzle size of 70 μ m at 4 °C to remove remaining contaminating CD31⁺ and CD45⁺ hematopoietic cells. The remaining cell population now entirely devoid of hematopoietic cell contamination was then sorted based on Sca-1. Sca-1⁺ MSC cells were collected. Sca-1⁻ cells were further sorted based on the marker CD51, and Sca-1⁻CD51⁺ cells were collected.

Culturing and Colony Formation of Sorted MSC and Progenitor Cells—Sca-1⁺ and Sca-1⁻CD51⁺ cells from wild-type and Y2^{-/-} mice were plated at a density of 1000 cells/well in 9.6-cm² plates (~ 100 cells/cm², BD Biosciences Labware) and cultured in control media (see section above) containing 20% fetal bovine serum, initially in 5% O₂/10% CO₂/85% N₂ (Air Liquide, Melbourne, Australia) at 37 °C for 3 days, then changed into regular culture conditions at 37 °C and 5% CO₂.

Formation of colonies by MSC and progenitor cells was assessed by evaluation of CFUs on day 7 of culture, when individual colonies were easily identifiable. Cells were initially fixed with 4% formaldehyde, washed with PBS, then stained with filtered (0.2- μ m filter, Sartorius, Hannover, Germany) 1% toluidine blue for 15 min at room temperature. The number of positively stained colonies containing >5 cells was counted for each experimental group.

Bone Densitometry—Bone mineral content (BMC) and bone mineral density (BMD) were measured in excised individual femora and tibia from 16-week-old Y1^{-/-} and wild-type mice, following collection and fixation in 4% paraformaldehyde for 16 h using a dedicated mouse dual x-ray absorptiometry (Lunar Piximus II, GE Medical Systems, Madison, WI). Scanning was performed with the knee joint in flexion to 90° to ensure consistent placement and scanning of the sagittal profile.

Statistical Analysis—Statistical differences in extent of mineralization or adipocyte differentiation based on values obtained from the image analysis software (Leica Microsystems), and analyses of BMD and BMC in Y1^{-/-} mice, were analyzed using two-tailed unpaired *t* tests between data from the two genotypes at equivalent time points using StatView version 4.5 (Abacus Concepts, San Francisco, CA). For all statistical analyses, *p* < 0.05 was accepted as being statistically significant.

RESULTS

Greater Mineralization and Adipocyte Formation in Cultured Stromal Cells from Germ Line Y2^{-/-} Mice—To examine whether bone cells from germ line Y2^{-/-} mice exhibit differences in proliferation and mineralization *in vitro*, we isolated bone marrow stromal cells from wild-type and germ line Y2^{-/-} mice and cultured them under osteogenic and adipogenic conditions to induce differentiation down the osteogenic and adipogenic lineages, respectively. Comparable numbers of cells were isolated from flushed bone marrow from wild-type and Y2^{-/-} mice (wild type, between 7.5×10^7 and 1.7×10^8 cells versus Y2^{-/-}, between 8 and 9.8×10^7 cells obtained from four bones per mouse) and were then plated at equal density. Viable cell numbers as assessed by trypan blue staining did not differ significantly between mutant and wild-type cultures in non-differentiating control conditions over a week in culture (data not shown), suggesting stromal cells from the two genotypes did not differ in their rate of proliferation.

A time-dependent increase in the extent of mineralization was revealed in von Kossa-stained osteogenic cultures, with a more marked accumulation of mineral in cultures from Y2^{-/-} mice compared with wild-type (Fig. 1A). These observations were confirmed by measurements of total mineral area by image analysis, with significantly greater mineralization measured in Y2^{-/-} cultures at days 18 and 21 (Fig. 1B). The pattern of mineralization also appeared to be more evenly distributed in the Y2^{-/-} cultures compared with wild-type cultures, in which mineral appeared to be more centrally localized (Fig. 1A), suggesting the presence of more mineral-producing osteoblastic cells throughout the Y2^{-/-} cultures. Increases in expression of the osteoblast marker genes alkaline phosphatase and osteocalcin at days 3 and 9 in Y2^{-/-} cultures supported these observations (Fig. 1C). Interestingly, under control culture conditions with no differentiation-inducing supplements in the media, von Kossa-positive mineral was observed in some wells from Y2^{-/-} but not wild-type mice (data not shown). These findings together suggest an increased capacity of osteoblastic cells from Y2^{-/-} mice to produce mineralized extracellular matrix *in vitro*.

Cells cultured under adipogenic conditions also showed elevated expression of peroxisome proliferator-activated receptor γ , a key regulator of adipocyte differentiation, in day 3 and day 9 Y2^{-/-} cultures (Fig. 1C), as well as a time-dependent increase in adipocyte differentiation, evidenced by Oil Red O staining, with a significantly greater number of adipocytes on days 18 and 21 of culture in cells from Y2^{-/-} compared with wild-type mice (Fig. 1, D and E). Thus, cultures of bone marrow cells from Y2^{-/-} mice exhibited an enhanced capability to undergo both osteoblast and adipocyte differentiation under appropriate cell culture conditions.

Because proliferation rates of cultures from the two genotypes were not different, the increased osteoblast mineralization and adipocyte number in cultures from Y2^{-/-} mice could be the result of intrinsic differences in the ability of progenitor cells to undergo osteoblast or adipocyte differentiation. Alternatively, because osteoblasts and adipocytes are derived from a common mesenchymal precursor, the differences observed in

Greater Osteoprogenitor Number of *Y2* Knockout Mice

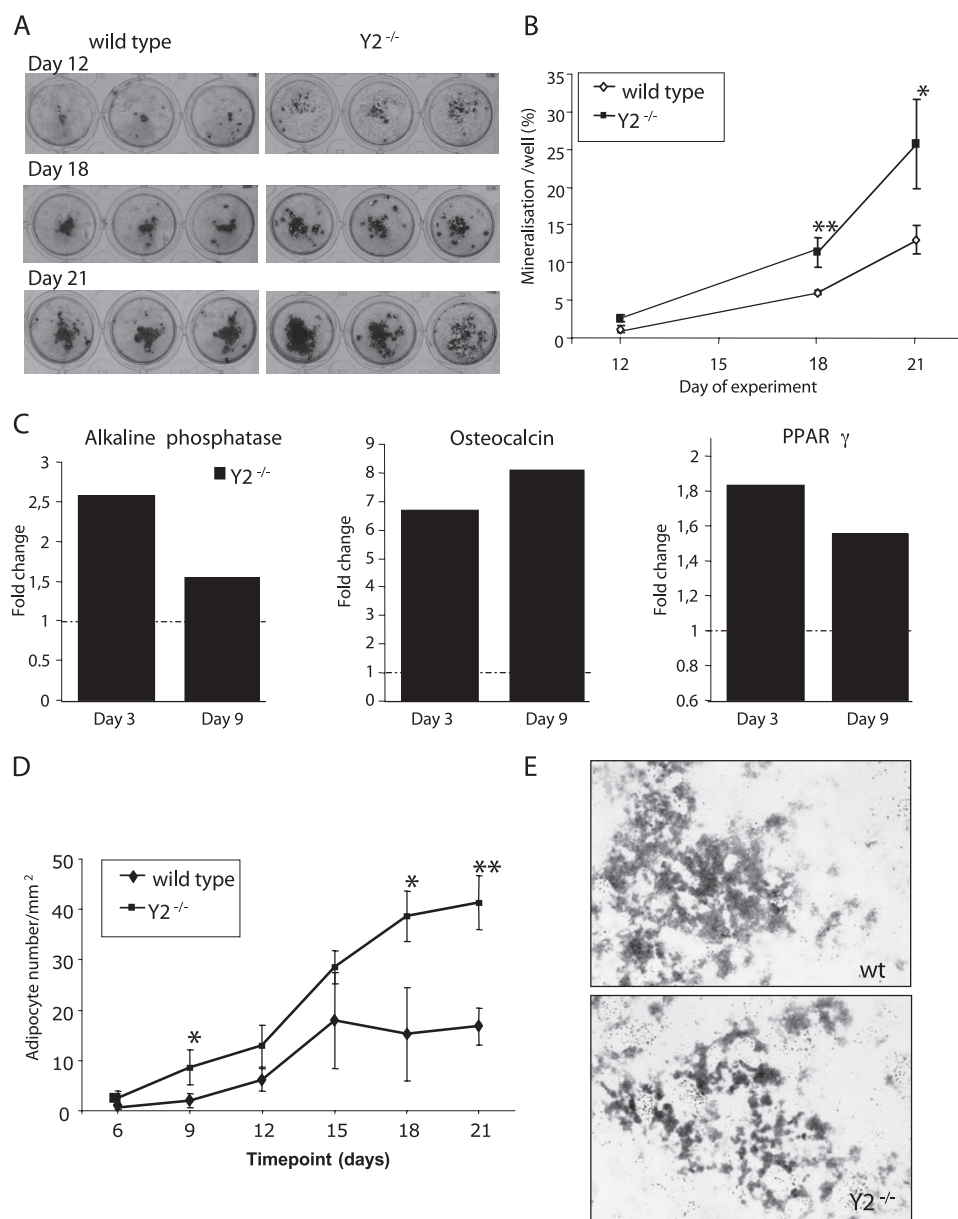


FIGURE 1. Stromal cells from *Y2*^{-/-} mice exhibit greater mineralization and adipocyte differentiation *in vitro*. A, von Kossa staining of mineral in stromal cell cultures from wild-type and *Y2*^{-/-} mice. B, quantification of mineral illustrates increased mineralization in *Y2*^{-/-} stromal cells cultured in osteogenic differentiation media. C, the graphs show -fold difference of the bone and adipocyte marker genes alkaline phosphatase, osteocalcin, and peroxisome proliferator-activated receptor γ ; greater expression of these genes in cultured stromal cells from *Y2*^{-/-} mice relative to wild-type (dotted lines) at days 3 and 9 of culture. D, adipocyte number was increased in *Y2*^{-/-} stromal cells cultured in adipogenic media. E, Oil Red O staining of cultured stromal cells shows greater adipocyte number in *Y2*^{-/-} cultures. *, $p < 0.05$; **, $p < 0.01$.

differentiation capability may result from a difference in the number of the common mesenchymal progenitors present within the bone of *Y2*^{-/-} mice.

Increased Numbers of Osteoprogenitor Precursors in Germ Line *Y2*^{-/-} Mice—Using FACS, two mesenchymal progenitor populations were isolated from wild-type and *Y2*^{-/-} mouse bones to investigate the proportion at which these cells were present in these genotypes. Previous studies have demonstrated that only a small percentage of the total number of mesenchymal progenitors are present within the bone marrow, with the majority of mouse mesenchymal cells present within compact

bone (25); consequently, MSCs and progenitor cells for these studies were isolated from compact bone tissue.

Consistent with the above results with flushed bone marrow, comparable numbers of cells were also prepared from compact bone of wild-type and *Y2*^{-/-} mice following collagenase digestion (wild-type, $4.9 \pm 0.38 \times 10^7$ cells versus *Y2*^{-/-}, $5.1 \pm 0.38 \times 10^7$ cells total from 10 mice, average cell numbers from three separate experiments). Importantly, although cell numbers decreased markedly following depletion of hematopoietic cells, the cell yields remained similar between the two genotypes (wild-type, $3.4 \pm 0.38 \times 10^6$ cells versus *Y2*^{-/-}, $3.5 \pm 0.38 \times 10^6$ cells total from 10 mice, average yield in three experiments). After further negative selection of CD45⁺ and CD31⁺ hematopoietic cells, the population was sorted based on the stem cell antigen Sca-1. Sca-1⁺ cells were gated and collected, whereas Sca-1⁻ cells were sorted again and a Sca-1⁻CD51⁺ cell population was gated and collected. Previous studies have established that Sca-1⁺ cells are immature mesenchymal stem cells (25, 28, 33), whereas Sca-1⁻CD51⁺ cells represent a more mature mesenchymal progenitor cell type.⁵

Numbers of Sca-1⁺ MSCs were comparable between wild-type and *Y2*^{-/-} mice, but there was a 2-fold greater number of Sca-1⁻CD51⁺ progenitor cells in bones from *Y2*^{-/-} compared with wild-type mice (Fig. 2). These findings suggest that the greater mineralization and adipocyte formation observed in the initial bone marrow stromal cell cultures from *Y2*^{-/-} mice was likely

due to a greater proportion of mature mesenchymal progenitor cells present at the initial plating.

Gene array analysis of the different subpopulations of Sca-1 cells confirmed the up/down-regulation of bone-specific genes further supporting a role of these cells in increased bone formation (supplemental Table S1).

The CFU assay is an indication of the relative abundance of proliferating progenitor cells within an isolated population

⁵ P. Simmons, unpublished data.

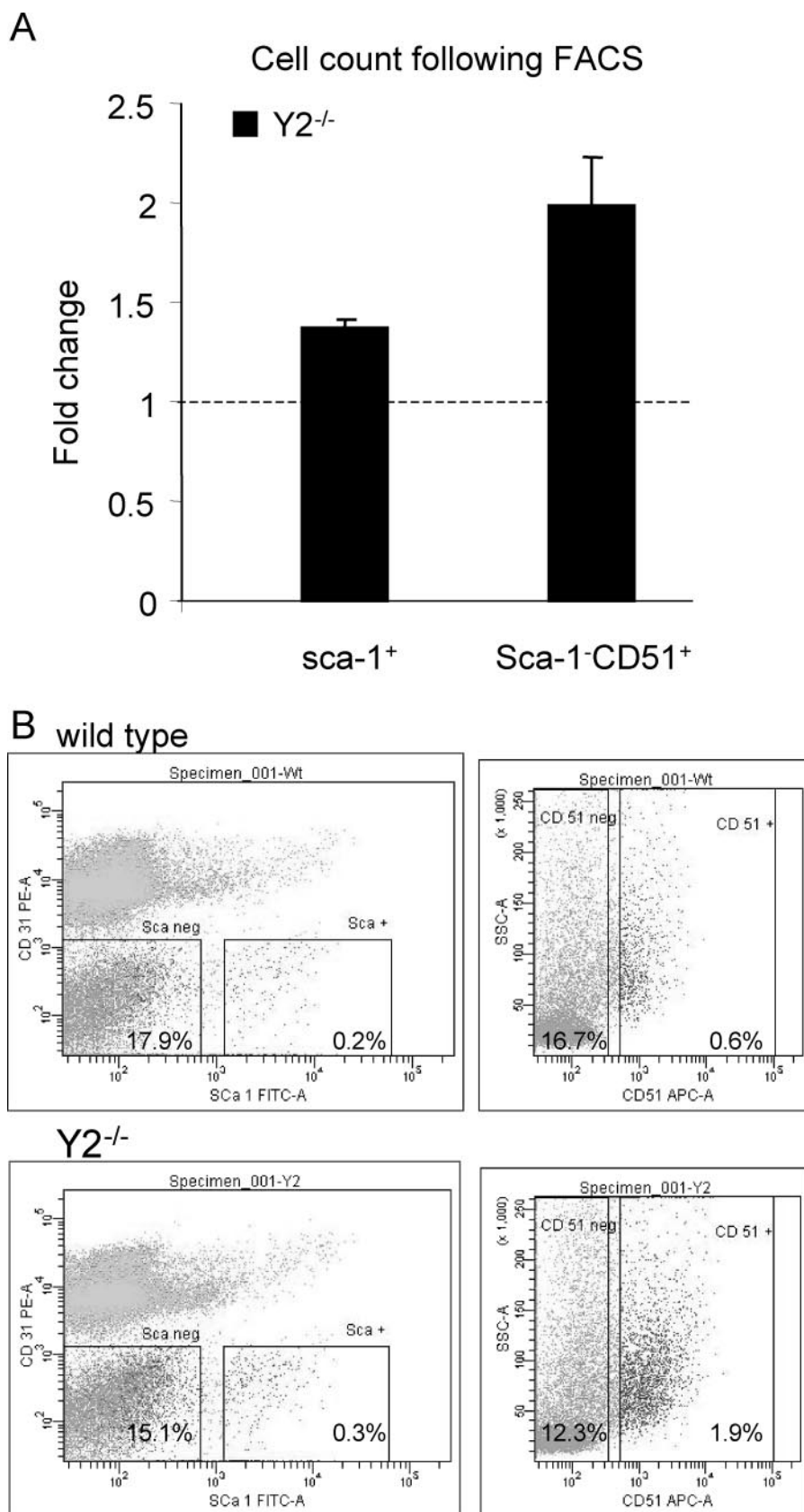


FIGURE 2. Greater number of mature mesenchymal progenitor cells present in bone of Y2^{-/-} mice. The -fold difference of Sca-1⁺ MSCs and Sca-1⁻CD51⁺ mature progenitor cells in Y2^{-/-} bone compared with wild-type (dotted line), average of three experiments (A), and proportion (B) of sorted populations in bones of wild-type and Y2^{-/-} mice (representative values from one of three experiments), shows a significant 2-fold increase in number of Sca-1⁻CD51⁺ progenitor cells in Y2^{-/-} bones ($p < 0.05$) but no difference in the number of Sca-1⁺ MSCs.

available for differentiation down the distinct mesenchymal lineages. Cells within the colonies from Sca-1⁺ and Sca-1⁻CD51⁺ cells were morphologically different, with a more fibroblastic appearance in the Sca-1⁺ cells and a more cuboidal morphology in Sca-1⁻CD51⁺ cultures, consistent with the proposed role of the latter population as a more mature osteoprogenitor cell type (Fig. 3A). Furthermore, CFU number was significantly greater in Sca-1⁺ compared with Sca-1⁻CD51⁺ cultures ($p < 0.001$), consistent with their proposed role as a more immature cell type. Importantly, however, there was no difference in CFU number or notable difference in the size of the individual colonies generated by either sorted cell type from wild-type and Y2^{-/-} mice (Fig. 3, B and C), suggesting that the abundance of progenitor cells within these populations was comparable between genotypes.

Y Receptor Expression in Bone Marrow Stromal Cells—To explore the molecular mechanism by which progenitor cell number might be increased in bones from Y2^{-/-} mice, the mRNA expression of different Y receptor transcripts in bone marrow stromal cell cultures from wt and Y2^{-/-} mice on day 3 and day 9 of culture was investigated. Expression of all Y receptor transcripts was detected in RNA isolated from brain tissue of wild-type mice using reverse transcription-PCR (Fig. 4A, and data not shown), confirming the ability of our primers to detect expression of the different Y receptor subtypes. Expression of Y1 mRNA was abolished in brains of Y1^{-/-} knock-out mice (Fig. 4A). Y1 receptor expression was also demonstrated in bone marrow stromal cell cultures from wild-type mice but was all but abolished in cultures from Y2^{-/-} mice (Fig. 4, B and C). This pattern was consistently observed in control, osteogenic, and adipogenic culture conditions. Expression of Y2, Y4, Y5, and Y6 receptors was not detected in stromal cells from either genotype (supplemental Fig. S1 and data not shown).

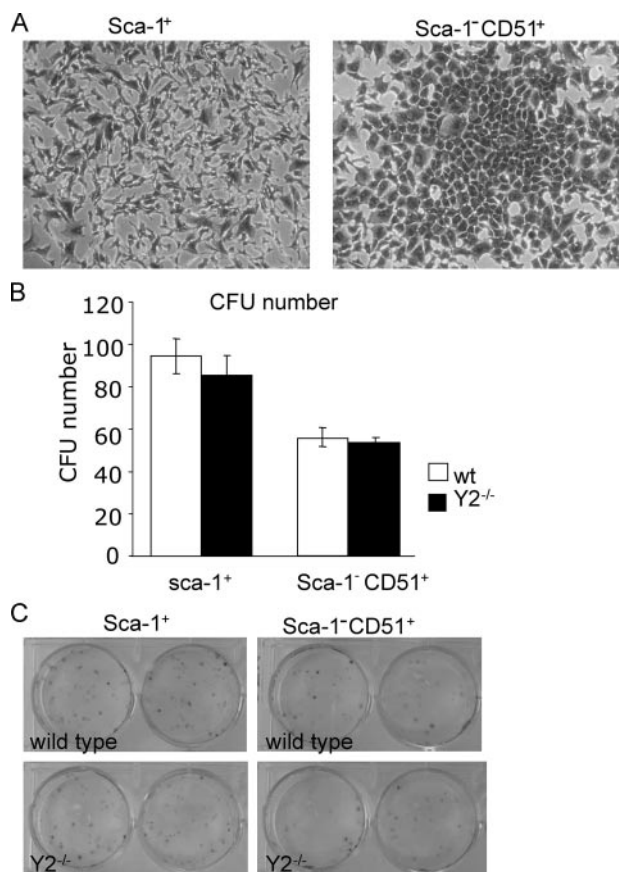


FIGURE 3. MSC and mature progenitor cells from wild-type and Y2^{-/-} mice are similar in their proliferative ability as assessed by numbers of CFUs. Difference in appearance of CFUs evident after toluidine blue staining at 100× magnification (A); CFU number after plating at equal density demonstrates no difference in CFU number between genotypes (B); overview of toluidine blue staining (C).

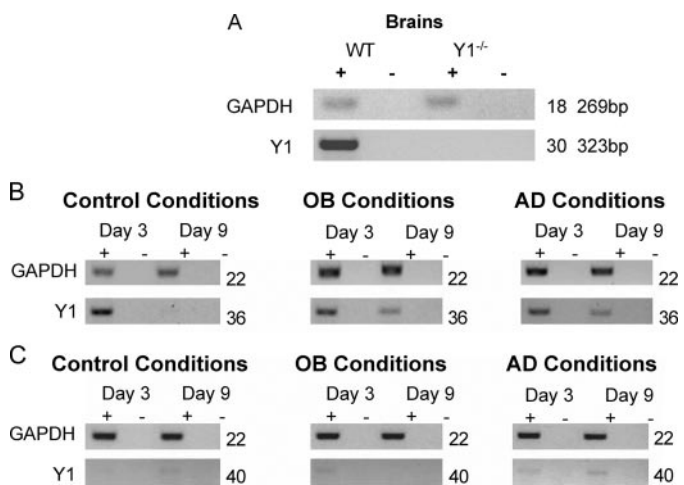


FIGURE 4. Y1 receptor is expressed in cultured bone marrow stromal cells from wild-type mice. Y1 receptor mRNA is detected in brain tissue of wild-type but not Y1^{-/-} mice (A). Y1 receptor is expressed in stromal cell cultures from wild-type mice at day 3 and 9 of culture under control, osteoblastic (OB), and adipocytic (AD) conditions (B), and is down-regulated at both these time points in stromal cells from Y2^{-/-} mice (C). Number of PCR cycles and product size are indicated. Data show results for PCR performed with (+) and without (-) reverse transcription.

Y1 Receptor Expression in Bone—Y1 receptor expression was also investigated in bone tissue using *in situ* hybridization. Y1 receptor gene transcripts were detected in osteoblasts on

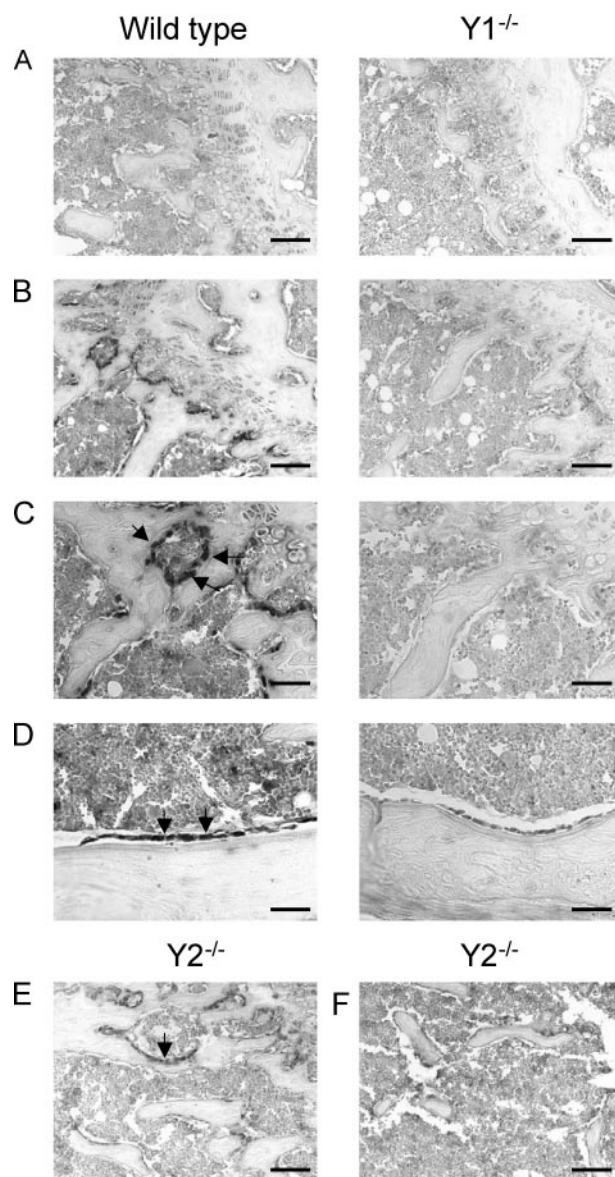


FIGURE 5. Y1 receptor expression in bone tissue. Analysis of Y1 receptor expression by *in situ* hybridization in wild-type, Y1^{-/-}, and Y2^{-/-} mice. A, B, E, and F, 20× magnification; C and D, 40× magnification. Sense probe negative control in wild-type and Y1^{-/-} mice shows no staining (A). Antisense staining of osteoblasts in trabecular and cortical bone of wild-type mice is absent in Y1^{-/-} mice (B–D). Y1 receptor expression is also associated with osteoblasts in bones from Y2^{-/-} mice (E), but sense probe-negative control in Y2^{-/-} mice again shows no staining (F). Arrows indicate Y1 receptor-positive osteoblasts. Bar, 50 μm (A, B, E, and F) and 12.5 μm (C and D).

endocortical and trabecular bone surfaces within the distal metaphysis of femurs from wild-type but not Y1^{-/-} mice (Fig. 5, A–D). Y1 receptor expression was also detected in osteoblastic cells of bones from Y2^{-/-} mice but appeared significantly down-regulated relative to expression in wild-type mice (Fig. 5, E and F). These findings together with the above data provide clear evidence for the expression of Y1 receptors by osteoblastic cells within bone tissue and *ex vivo*.

Greater Bone Density in Y1^{-/-} Mice—The presence of Y1 receptors on osteoblasts within bone tissue and their down-regulation following Y2 receptor deletion suggest a key role for local Y1 receptor signaling in the control of bone formation. To

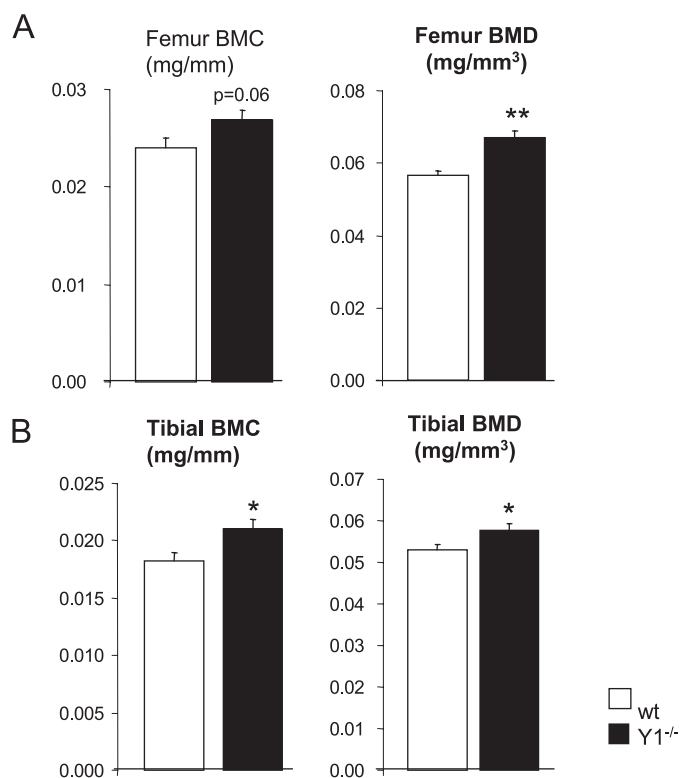


FIGURE 6. Greater bone mineral content and density in $Y1^{-/-}$ mice. Analysis of BMC and BMD in the femora (A) and tibiae (B) of wild-type and $Y1^{-/-}$ mice, reveals greater femoral BMD and tibial BMC and BMD in $Y1^{-/-}$ mice compared with wild-type. *, $p < 0.05$; **, $p < 0.01$. Number of bones analyzed per group, 8–10.

investigate the effect of altered Y1 receptor signaling on bone mass *in vivo*, femora and tibia from germ line $Y1^{-/-}$ mice were assessed for changes in BMC and BMD. Consistent with an inhibitory role of Y1 signaling on bone formation, femoral BMD was significantly greater in $Y1^{-/-}$ mice compared with wild type, with a similar trend in femoral BMC (Fig. 6A). Similarly, in the tibiae, both BMC and BMD were significantly elevated in $Y1^{-/-}$ mice compared with wild type (Fig. 6B), demonstrating the ability of altered Y1 receptor signaling to alter bone formation.

DISCUSSION

The findings presented here demonstrate that adherent bone marrow stromal cells from $Y2^{-/-}$ mice have an enhanced ability to differentiate down osteoblastic and adipocytic lineages compared with wild-type stromal cells *in vitro*. Analysis of the population of mesenchymal progenitors within the bones of these mice revealed a 2-fold greater number of mesenchymal progenitor cells in $Y2^{-/-}$ compared with wild-type mice. After plating the immature Sca-1⁺ MSCs and the more mature Sca-1⁻ CD51⁺ cells from the wild-type and $Y2^{-/-}$ mice at the same density, however, the number and sizes of colonies formed were similar between the two genotypes, indicating that these cells of the two mouse genotypes were comparable in their colony-forming ability and, therefore, most likely also in their differentiation potential. Together these findings suggest that a change in the size of a multipotential mesenchymal progenitor population may be a contributing mechanism for the greater bone mass of $Y2^{-/-}$ mice.

The greater mineralization seen in $Y2^{-/-}$ stromal cell cultures *in vitro* is consistent with the greater bone formation and bone volume of the $Y2^{-/-}$ model *in vivo*. In contrast, the enhanced adipocytic differentiation capacity was initially surprising, because the $Y2^{-/-}$ mice have a lean phenotype, with reduced white adipose mass compared with wild-type animals (34) and a trend for reduced numbers of marrow adipocytes (wild-type, 5.5 ± 1.0 versus $Y2^{-/-}$, 2.3 ± 1.2 adipocytes per distal femur 5- μ m sagittal section, $p = 0.09$). However, the greater number of mature multipotential progenitors in $Y2^{-/-}$ bones is consistent with an enhanced ability of cultured stromal cells from $Y2^{-/-}$ mice to differentiate down either the osteoblastic or the adipocytic lineage under appropriate culture conditions. Thus, unlike the consistent positive effects of Y2 receptor gene deletion on the osteogenic cell lineage *in vitro* and *in vivo*, the greater adipocytic differentiation in $Y2^{-/-}$ cells observed *in vitro* does not necessarily reflect the *in vivo* situation.

To date, there is no standard method for the isolation of murine mesenchymal stem or progenitor cells. Different approaches have yielded populations of cells with variability in their proliferative and differentiative capacities (24, 26–28, 33, 35–37). In the present study, a purified hematopoietic-depleted cell population was further divided into immature MSC and mature progenitor cells based on the presence or absence of Sca-1. Sca-1 is a cell surface glycoprotein commonly used as a marker for the isolation of hematopoietic stem cells from mouse bone marrow. Although the physiological role of Sca-1 in the hematopoietic lineage is incompletely understood, its presence appears to be required for normal hematopoietic stem cell activity and lineage fate, and possibly also for the appropriate self-renewal and homing ability of hematopoietic stem cells (38, 39). Importantly, however, Sca-1 is also expressed on non-hematopoietic bone marrow stromal cells, and mice lacking Sca-1 develop late-onset osteoporosis due to a deficiency in osteoprogenitor cells (40). Therefore, Sca-1 expression also appears to be required for the appropriate self-renewal of mesenchymal progenitors and identifies a population of immature mesenchymal cells with the ability to undergo osteoblast differentiation. The Sca-1⁺ cell population isolated from bone following depletion of hematopoietic cells, which represent an immature multipotential cell type, did not differ between $Y2^{-/-}$ mice and wild-type mice. The number of Sca-1⁻ CD51⁺ mature progenitor cells, however, was 2-fold greater in bones from $Y2^{-/-}$ mice relative to wild type. The greater number of these more mature progenitor cells provides a likely mechanism by which mineralization and adipogenesis were increased in stromal cell cultures from $Y2^{-/-}$ mice compared with wild-type. These findings support the likelihood that an increase in the progenitor population may contribute to the increased bone formation and volume of $Y2^{-/-}$ mice *in vivo*.

Previous studies have demonstrated the presence of NPY-immunoreactive fibers in periosteum and bone marrow and associated with bone lining cells *in vivo* (3, 41). Also, administration of NPY inhibited the cAMP response to parathyroid hormone and norepinephrine in some osteoblastic cell lines *in vitro* (4, 42), suggesting the presence of functional NPY receptors on bone cells and a possible role for NPY in the regulation

of osteoblast activity. Our evaluation of the expression of the different Y receptors in cultures of bone marrow stromal cells from wild-type and $Y2^{-/-}$ mice under different differentiation conditions revealed high levels of Y1 receptor expression in wild-type cultures under normal, osteogenic, and adipogenic conditions. Furthermore, expression of Y1 receptor in osteoblasts on endocortical and trabecular bone surfaces within femur bone tissue was detected using *in situ* hybridization, providing supporting evidence for the presence of Y1 receptors on bone forming cells.

The observation that Y1 receptor expression was virtually abolished in cultures from $Y2^{-/-}$ mice suggests that reduced Y1 receptor signaling in the bone microenvironment is important for the anabolic bone phenotype of the $Y2^{-/-}$ model. Importantly, these studies also revealed that germ line deletion of Y1 receptors resulted in greater BMD and BMC *in vivo*. Further characterization of this model has demonstrated the greater bone volume of the $Y1^{-/-}$ model to be the result of a greater rate of bone formation, which, unlike the $Y2^{-/-}$ model, does not appear to be regulated via a central mechanism (see accompanying report (46)). The direct linkage of hypothalamic to peripheral changes in osteoblast activity has also been described in leptin-deficient *ob/ob* mice. In that model central leptin signaling within the hypothalamus has a direct neural connection to osteoblasts via sympathetic neurons, which alter osteoblast activity by modulation of β_2 adrenergic receptors expressed on these cells (19). In a similar manner, central Y2 signaling may regulate osteoblast activity by NPY-ergic neuronal modulation of osteoblastic Y1 receptors. Although these two pathways appear to have separate mechanisms, interaction between the Y2 and leptin pathways is still an open question. Interestingly, consistent with this possibility, $Y2^{-/-}/ob$ double knock-out mice do not show additive effects on bone formation (43). It is plausible that deletion of Y2 receptors either directly or indirectly leads to a change in Y1 receptor mRNA expression in bone, with downstream consequences on osteoblast activity.

Altered expression of remaining Y receptors within certain brain regions has been observed in germ line Y receptor knock-out models, indicative of cross-regulation between different Y receptors or overlapping functions in different signaling pathways (44). In the $Y2^{-/-}$ model, it is likely that the lack of Y2 receptor signaling mediates the down-regulation of Y1 receptors in osteoblast precursors, because the evidence from the present study indicates a lack of Y2 receptor mRNA in bone cells. Y2 receptors are known to be expressed on the pre-synaptic side of sympathetic nerve terminals and act in an autoinhibitory fashion to regulate the release of NPY and other neurotransmitters (45). The lack of this feedback inhibition on NPY release could lead to elevated levels of NPY, which in turn might then cause an overstimulation of Y1 receptors on bone precursor cells, and subsequently to desensitization and down-regulation of this Y1 receptor population. This would also be consistent with the increased bone formation observed after hypothalamus-specific Y2 receptor deletion, whereby sympathetic nervous activity is potentially altered, thereby leading to increased transmitter release (including NPY) in the periphery and causing a similar down-regulation of Y1-receptors on bone forming cells. This is supported by a recent study, which used

pseudorabies virus-based transneuronal tracing to map transsynaptically connected neurons from rat bone providing direct evidence that nerve fibers within bone tissue are under the control of synaptic transmission from the hypothalamus (5). However, it cannot be excluded that part of the effect on Y1-receptor down-regulation is due to NPY produced by cells such as megakaryocytes within the bone marrow itself (6).

In summary, we have shown here that the NPY system plays an important part in the differentiation and proliferation of osteoblastic and adipocytic lineages, with a greater number of mesenchymal progenitor cells present in bones from $Y2^{-/-}$ mice. The likely mechanism leading to greater bone formation in $Y2^{-/-}$ mice appears to be due to increased NPY levels and subsequent down-regulation of Y1 receptors on bone cells. Initial studies presented in this report suggest a key role for local Y1 receptor signaling in the control of osteoblast activity. These findings together identify potential new avenues for the treatment and prevention of bone loss. For a much more detailed characterization of the role of Y1 receptors and their interaction with Y2 receptors in the control of bone formation, the reader is referred to the accompanying report (46).

Acknowledgments—We thank Julie Wheway for help with the cell sorting, Leah Worton for help establishing stromal cell culture methods, Jerome Darakdjian for operating the cell sorter, and Prof. Ulf Lerner, Dept. of Oral Cell Biology, Umeå University, for kindly providing access to the real-time PCR facility.

REFERENCES

- Baldock, P. A., Sainsbury, A., Couzens, M., Enriquez, R. F., Thomas, G. P., Gardiner, E. M., and Herzog, H. (2002) *J. Clin. Invest.* **109**, 915–921
- Baldock, P. A., Allison, S. J., McDonald, M. M., Sainsbury, A., Enriquez, R., Little, D. G., Eisman, J. A., Gardiner, E. M., and Herzog, H. (2006) *J. Bone Miner. Res.* **21**, 1600–1607
- Hill, E. L., Turner, R., and Elde, R. (1991) *Neuroscience* **44**, 747–755
- Bjurholm, A. (1991) *Int. Orthop.* **15**, 325–329
- Denes, A., Boldogkoi, Z., Uhereczky, G., Hornyak, A., Rusvai, M., Palkovits, M., and Kovacs, K. J. (2005) *Neuroscience* **134**, 947–963
- Ericsson, A., Schalling, M., McIntyre, K. R., Lundberg, J. M., Larhammar, D., Seroogy, K., Hokfelt, T., and Persson, H. (1987) *Proc. Natl. Acad. Sci. U. S. A.* **84**, 5585–5589
- Bjurholm, A., Kreicbergs, A., Terenius, L., Goldstein, M., and Schultzberg, M. (1988) *J. Auton. Nerv. Syst.* **25**, 119–125
- Ahmed, M., Bjurholm, A., Kreicbergs, A., and Schultzberg, M. (1993) *Spine* **18**, 268–273
- Lindblad, B. E., Nielsen, L. B., Jespersen, S. M., Bjurholm, A., Bunger, C., and Hansen, E. S. (1994) *Acta Orthop. Scand.* **65**, 629–634
- Sisask, G., Bjurholm, A., Ahmed, M., and Kreicbergs, A. (1996) *J. Auton. Nerv. Syst.* **59**, 27–33
- Mullins, M. W., Ciallella, J., Rangnekar, V., and McGillis, J. P. (1993) *Regul. Pept.* **49**, 65–72
- Togari, A., Arai, M., Mizutani, S., Mizutani, S., Koshihara, Y., and Nagatsu, T. (1997) *Neurosci. Lett.* **233**, 125–128
- Cornish, J., Callon, K. E., Lin, C. Q., Xiao, C. L., Gamble, G. D., Cooper, G. J., and Reid, I. R. (1999) *J. Bone Miner. Res.* **14**, 1302–1309
- Goto, T., Yamaza, T., Kido, M. A., and Tanaka, T. (1998) *Cell Tissue Res.* **293**, 87–93
- Mori, T., Ogata, T., Okumura, H., Shibata, T., Nakamura, Y., and Kataoka, K. (1999) *Biochem. Biophys. Res. Commun.* **262**, 418–422
- Lundberg, P., Bostrom, I., Mukohyama, H., Bjurholm, A., Smans, K., and Lerner, U. H. (1999) *Regul. Pept.* **85**, 47–58
- Lundberg, P., Lie, A., Bjurholm, A., Lehenkari, P. P., Horton, M. A., Lerner,

- U. H., and Ransjo, M. (2000) *Bone* **27**, 803–810
18. Lundberg, P., Lundgren, I., Mukohyama, H., Lehenkari, P. P., Horton, M. A., and Lerner, U. H. (2001) *Endocrinology* **142**, 339–347
 19. Takeda, S., Eleftheriou, F., Levasseur, R., Liu, X., Zhao, L., Parker, K. L., Armstrong, D., Ducey, P., and Karsenty, G. (2002) *Cell* **111**, 305–317
 20. Moore, R. E., Smith, C. K., Bailey, C. S., Voelkel, E. F., and Tashjian, A. H. (1993) *Bone Miner.* **23**, 301–315
 21. Kellenberger, S., Muller, K., Richener, H., and Bilbe, G. (1998) *Bone* **22**, 471–478
 22. Beresford, J. N., Bennett, J. H., Devlin, C., Leboy, P. S., and Owen, M. E. (1992) *J. Cell Sci.* **102**, 341–351
 23. Nuttall, M. E., Patton, A. J., Olivera, D. L., Nadeau, D. P., and Gowen, M. (1998) *J. Bone Miner. Res.* **13**, 371–382
 24. Pittenger, M. F., Mackay, A. M., Beck, S. C., Jaiswal, R. K., Douglas, R., Mosca, J. D., Moorman, M. A., Simonetti, D. W., Craig, S., and Marshak, D. R. (1999) *Science* **284**, 143–147
 25. Short, B., Brouard, N., Occhiodoro-Scott, T., Ramakrishnan, A., and Simmons, P. J. (2003) *Arch. Med. Res.* **34**, 565–571
 26. Baddoo, M., Hill, K., Wilkinson, R., Gaupp, D., Hughes, C., Kopen, G. C., and Phinney, D. G. (2003) *J. Cell. Biochem.* **89**, 1235–1249
 27. Wiczorek, G., Steinhoff, C., Schulz, R., Scheller, M., Vingron, M., Ropers, H. H., and Nuber, U. A. (2003) *Cell Tissue Res.* **311**, 227–237
 28. Van Vlasselaer, P., Falla, N., Snoeck, H., and Mathieu, E. (1994) *Blood* **84**, 753–763
 29. Howell, O. W., Scharfman, H. E., Herzog, H., Sundstrom, L. E., Beck-Sickingler, A., and Gray, W. P. (2003) *J. Neurochem.* **86**, 646–659
 30. Sainsbury, A., Schwarzer, C., Couzens, M., Fetisov, S., Furtinger, S., Jenkins, A., Cox, H. M., Sperk, G., Hokfelt, T., and Herzog, H. (2002) *Proc. Natl. Acad. Sci. U. S. A.* **99**, 8938–8943
 31. Schwenk, F., Baron, U., and Rajewsky, K. (1995) *Nucleic Acids Res.* **23**, 5080–5081
 32. Parker, R. M., and Herzog, H. (1999) *Eur. J. Neurosci.* **11**, 1431–1448
 33. Miura, Y., Miura, M., Gronthos, S., Allen, M. R., Cao, C., Uveges, T. E., Bi, Y., Ehrhchiou, D., Kortessidis, A., Shi, S., and Zhang, L. (2005) *Proc. Natl. Acad. Sci. U. S. A.* **102**, 14022–14027
 34. Sainsbury, A., Baldock, P. A., Schwarzer, C., Ueno, N., Enriquez, R. F., Couzens, M., Inui, A., Herzog, H., and Gardiner, E. M. (2003) *Mol. Cell Biol.* **23**, 5225–5233
 35. Prockop, D. J. (1997) *Science* **276**, 71–74
 36. Kitano, Y., Radu, A., Shaaban, A., and Flake, A. W. (2000) *Exp. Hematol.* **28**, 1460–1469
 37. Phinney, D. G., Kopen, G., Isaacson, R. L., and Prockop, D. J. (1999) *J. Cell. Biochem.* **72**, 570–585
 38. Ito, C. Y., Li, C. Y., Bernstein, A., Dick, J. E., and Stanford, W. L. (2003) *Blood* **101**, 517–523
 39. Bradfute, S. B., Graubert, T. A., and Goodell, M. A. (2005) *Exp. Hematol.* **33**, 836–843
 40. Bonyadi, M., Waldman, S. D., Liu, D., Aubin, J. E., Grynopas, M. D., and Stanford, W. L. (2003) *Proc. Natl. Acad. Sci. U. S. A.* **100**, 5840–5845
 41. Ahmed, M., Srinivasan, G. R., Theodorsson, E., Bjurholm, A., and Kreicbergs, A. (1994) *Regul. Pept.* **51**, 179–188
 42. Bjurholm, A., Kreicbergs, A., Schultzberg, M., and Lerner, U. H. (1992) *J. Bone Miner. Res.* **7**, 1011–1019
 43. Baldock, P. A., Sainsbury, A., Allison, S., Lin, D., Couzens, M., Boey, D., Enriquez, R. F., Durning, M., Herzog, H., and Gardiner, E. M. (2005) *J. Bone Miner. Res.* **20**, 1851–1857
 44. Lin, S., Boey, D., Couzens, M., Lee, N., Sainsbury, A., and Herzog, H. (2005) *Neuropeptides* **39**, 21–28
 45. King, P. J., Williams, G., Doods, H., and Widdowson, P. S. (2000) *Eur. J. Pharmacol.* **396**, R1–R3
 46. Baldock, P. A., Allison, S. J., Lundberg, P., Lee, N. J., Slack, K., Lin, E.-J. D., Enriquez, R. F., McDonald, M. M., Zhang, L., Durning, M. J., Little, D. G., Eisman, J. A., Gardiner, E. M., Yulyaningsih, E., Lin, S., Sainsbury, A., and Herzog, H. (2007) *J. Biol. Chem.* **282**, 19092–19102